Paleoceanography, **14**, 422–429, 1999

Error analysis of paleosalinity calculations

Gavin A. Schmidt
NASA Goddard Institute for Space Studies and Center for Climate Systems Research
Columbia University, New York

Abstract

A detailed error analysis is performed for the calculation of open-ocean salinity changes from carbonate oxygen-18 proxy data. Measurement errors are generally negligible, however, errors due to the "goodness of fit" of various regressions used in the calculation are significant. Depending on the method used and on the proxies available, error bars (1σ) for the salinity range from 0.6 to 1.8. In particular, expected errors for the midlatitude and tropical salinity differences at the Last Glacial Maximum are around 1.1 to 2.5. The largest errors occur because of the differences between temporal and spatial seawater oxygen-18:salinity relationships and through the use of nonconcurrent temperature measurements. Methods of improving paleosalinity estimates should focus on eliminating these large sources of uncertainty.

1. Introduction

Many methods now exist for estimating paleotemperatures including transfer functions, modern analogs, alkenone ratios, ratios of Sr/Ca (in aragonite) and, more recently, of Mg/Ca (in calcite). This has led to the hope that carbonate oxygen-18 (δ_c) records can be adjusted for local temperature changes and used to produce seawater oxygen-18 (δ_w) records, which in turn, it is assumed, can be related to paleosalinity.

Such surface paleosalinity reconstructions are becoming part of the standard paleoclimatic toolbox. However, the use to which a paleorecord can be put is heavily associated with its accuracy. This approach calculates paleosalinity indirectly as a residual, and hence particular care must be taken to estimate the errors in such calculations before any paleoclimatic conclusions are drawn. In previous work, error bars have generally only been given for some of the more obvious errors and rarely combined correctly to give the overall error estimate.

The relationship between oxygen-18 and salinity is fundamental to this calculation since it used in calibrations to present-day conditions and in the final deduction of the paleosalinity record. With more recent observations of seawater oxygen-18 and the advent of atmosphere and ocean general circulation models that contain the physics necessary to calculate oxygen-18 ratios in water a better understanding of this relationship is becoming clear. Hence the scatter associated with this relationship (the "goodness of fit") and its change through time can be used to estimate errors associated with its use.

Since these errors were not previously considered (perfect correlations and invariance through time were assumed) they have the effect of increasing the error bars previously published. However, since most of the previously implicit errors are now clear it should henceforth become easier to concentrate efforts on eliminating the most significant.

2. Oxygen-18/Salinity Relationship

Observations [*Craig and Gordon*, 1965; *Östlund et al.*, 1987; *Fairbanks et al.*, 1992; *Bauch et al.*, 1995] and modeling studies [*Schmidt*, 1998, ; G.A. Schmidt, Forward modeling of carbonate proxy data from planktonic foraminifera using oxygen isotope tracers in a global ocean model, submitted to *Paleoceanography*, 1999, hereinafter referred to as Schmidt, submitted manuscript, 1999] have all demonstrated that the surface ocean values of salinity and δ_w are roughly linearly related. How rough is this relationship? Depending on the scale over which the data is examined the answer varies. For all upper ocean (<250 m) samples from Geochemical Ocean Sections Study (GEOSECS) (including H. Craig, unpublished data, 1987) the relationship, given that the errors in measurements of salinity ($\sim$0.002) are much smaller than the errors in δ_w ($\sim$0.05‰), is

$$\delta_w = -17.0 + 0.495S \pm \sigma_{\rm ml} \qquad (1)$$

(r^2=0.88, δ_w defined with respect to Vienna SMOW). The 95% confidence limits on the intercept value and gradient are small ($\pm$0.2 and $\pm$0.006, respectively). The standard error $\sigma_{\rm ml}$ of δ_w (for known S) from this relationship is 0.2‰. Conversely, for known δ_w, the standard error in S is 0.4. This is explicitly included in (1) to emphasize goodness of fit as a separate source of error. Models show approximately the same degree of global scatter. However, at the regional scale in both models (Figure 1) and observations, there can be wide variations in the mixing lines. For instance, scatter in a collection of tropical samples [*Craig and Gordon*, 1965; *Östlund et al.*, 1987; *Duplessy et al.*, 1981, ; R. G. Fairbanks, unpublished data, 1998] is 0.13‰ (with slope 0.30) In the Arctic it can be as high as 0.3‰ (slope 1.02) [*Bauch et al.*, 1995]. The global mixing line is thus most appropriate for the midlatitudes to high latitudes; in other regions the local mixing line should be considered.

Figure 1

The temporal relationships (how δ_w:S varies with time at a point) on seasonal, interannual, or longer timescales are not as well defined. The observations of seasonal variability in δ_w are few and mainly confined to the tropical Pacific [*Wellington et al.*, 1996, ; R. G. Fairbanks, unpublished data, 1998], and coastal regions such as the Gulf of Maine [*Fairbanks*, 1982]. These observations hint that at least seasonally, spatial relationships change as a function of the isotopic content of the dominant freshwater sources (for instance, river outflow off Maine). Modeling studies also seem to indicate large seasonal excursions, especially in the Southern Oceans where there is a large sea ice meltwater signal. This meltwater consists of seawater that was frozen in the open ocean (enriched by $\sim$3‰ over the seawater from which it derives), highly depleted snow (-15–-20‰), and snow-ice made from snow and sea water frozen in situ [*Macdonald et al.*, 1995]. The proportions of these types of ice vary depending on location and season (for instance, snow-ice is more prevalent in the Southern Ocean). The

salinity of sea ice varies from ∼13 for newly formed ice, to below 5 for multiyear ice. Hence the isotopic and salt content of sea ice meltwater and its influence on the δ_w:S relationship can vary greatly. More observations and better constrained models are necessary to completely quantify these effects. Thus it can be expected that the error involved in estimating δ_w from the salinity is a function of season, but this should not significantly increase the absolute error. Since most regional surface relationships tend to converge near δ_w=0.8‰ and S=36. errors in using an incorrect linear relationship will tend to be greater at low salinities.

There is no evidence that long-term changes in δ_w:S parallel the spatial relationship. Given the scatter in the δ_w:S plane, it is more than likely that for small changes in δ_w (<0.2%), there is little or no correlation with salinity. Model results (Figure 2) demonstrate that although there is a tendency for the larger changes to be associated with the linear relation, smaller changes in salinity are unrelated to those in δ_w. This would seem to be a fundamental constraint on the application of this methodology.

In the case where there has been a significant change in climate the slope of the linear regressions might also change. For the global regression the change could be estimated by assuming that the high-latitude end-member of precipitation was different and that the linear regression still passed through the ocean mean point (currently δ_w=0‰, S=34.7), which it does at present within $1\sigma_{\rm ml}$). This assumption is probably better than assuming no change through time and, indeed, a thorough investigation of δ_w:S changes in a recent study [*Rohling and Bigg*, 1998] concluded that the global mixing line is unlikely to have remained the same under the very different hydrologic conditions pertaining at the Last Glacial Maximum (LGM).

At a regional level it is much more difficult to determine the temporal variation of the mixing line. For instance, *Rohling and Rijk* [1999] provide good evidence that the Mediterranean has experienced large changes in the hydrologic cycle through time that significantly changed the regional mixing line. Model results may be of help in determining these changes and possibly the degree to which the ratios of evaporation to precipitation/runoff may vary. In the tropics the mean freshwater end-member will always be close to the average tropical evaporation (since most rain is not exported to the higher latitudes). However, changes in water transport in the atmosphere could lead to substantially different variations in different oceans. A greater regional evaporation to precipitation ratio (E/P) will imply a shallowing of the mixing line, smaller E/P will imply a steepening. However, the tropical mixing lines do not pass through ocean mean water, and so, another assumption has to be made concerning the relationship of the regional waters to the global mean.

3. Methodologies and Error Estimates

This section outlines the steps involved in the most general way possible. There is generally some freedom in how to proceed and for some methodologies some steps are unnecessary and can be bypassed. For each step a conservative error estimate is derived that depends on the particular choices that could be made. Errors are of three forms: measurement errors (usually small), uncertainties in derived coefficients, and scatter. Error estimates are given in terms of the standard error σ, which implies that 67% of the data lie with $\pm\sigma$ of the mean.

These errors can propagate through the process. The error in the final product can be calculated from the following formula: if $Y = f(X_1, X_2, \ldots, X_n)$ and each of the X_I has a standard error σ_{X_i} associated with it, then the standard error of Y, σ_Y, can be written as [*Press et al.*, 1990]

$$\sigma_Y^2 = \sum_{i=1}^{n} \left(\frac{\partial f}{\partial X_i} \right)^2 \sigma_{X_i}^2 \qquad (2)$$

Systematic errors in constant intercepts are ignored in the subsequent calculations since it is anticipated that changes of δ_w and S, not absolute values, will be considered most important. Differences have a slightly higher scatter than absolute values by a factor of $\sqrt{2}$.

3.1. Retrieve a Record of δ_c Through Time

The error σ_c in δ_c in foraminifera depends mainly on the number of shells analyzed, and for standard practice this has an associated error of around 0.1‰ [*Duplessy et al.*, 1991]. In corals, reproducibility is better, and errors are around 0.06‰ [*Wellington et al.*, 1996].

3.2. Retrieve an Independent Temperature Proxy T_p

A temperature proxy is usually calibrated to seasonal or annual mean sea surface temperature (SST), and each proxy comes with its own error. Commonly

used proxies have approximately standard errors σ_{T_p} of ± 1°C (including alkenone and coral Sr/Ca ratios [*Muller et al.*, 1998; *Gagan et al.*, 1998]). Faunal assemblages or modern analog methods claim similar accuracy (± 1.9°C and ± 1.5°C, respectively [*Ortiz and Mix*, 1997]), but given the debate over the tropical temperatures at the LGM, this may be an underestimate. Mg/Ca ratios are more experimental, and preliminary estimates of the precision and reproducibility errors lead to temperature errors of ~ 1.3°C [*Hastings et al.*, 1998]. Note that these errors are not necessarily typical of all situations where these proxies may be used: representative errors should be calculated for each separate application.

3.3. Choose a Paleotemperature Equation

Equations derived from inorganic data [*O'Neil et al.*, 1969] have traditionally been used to determine the temperature-dependent fractionation at calcification. However, recent experiments with inorganic carbonate at lower temperatures [*Kim and O'Neil*, 1997] and with cultured foraminifera [*Spero et al.*, 1997; *Bemis et al.*, 1998] have produced discrepancies with the earlier equations. The differences can be as large as 4°C over the range 0°– 25°C [*Bemis et al.*, 1998] (maximum differences are for cooler temperatures). As an example, the linear fit to the *Kim and O'Neil* [1997] data is

$$T = A + B(\delta_c - \delta_w) \pm \sigma_T \qquad (3)$$

with $A = 16.3$ and $B = -5.0$ (δ_c and δ_w are defined with respect to Peedee Belemnite (PDB)) and has an error $\sigma_T = 0.8$°C (essentially the same as for a quadratic approximation). For corals, there are species-dependent "vital" effects that cause the temperature dependence to vary [*Weber and Woodhead*, 1972]. Scatter around the linear regressions typically has an error $\sigma_T = 0.5$°C [*Gagan et al.*, 1998].

The values of the slope B in other equations range from -4 to -5. Hence error in the gradient (σ_B) of ~ 0.3 could also be included in the error analysis. However, the scatter amongst different paleotemperature equations is not a normally distributed random variable, and it is unclear how to treat it. However, for both corals and foraminifera, differences in possible equations are mainly in the intercept, rather than the slope, and hence temperature differences are better constrained than absolute values.

3.4. Calibrate the Calcification Temperatures T_c and Those Measured by the Proxy

This step is necessary only when the proxy temperature is distinct in season and/or environment from the calcification of the carbonate, for instance, when using faunal assemblage transfer functions or alkenone ratios to estimate annual mean or summer SST. Ratios of Mg/Ca or Sr/Ca, however, should record the temperature concurrently at calcification and could be used directly in (3), provided that the calibration of these proxies is done to the in situ temperature and not to the summer SST or some such variable.

The calcification temperature is calculated from (3). For that the present-day distribution of δ_w at calcification must be estimated. In the general absence of any concurrent δ_w measurements at core sites to compare with the core-top δ_c values, δ_w is usually estimated from either a local or global δ_w:S relationship. As described above, the standard error $\sigma_{\rm ml}$ in doing so in the open ocean is probably ~ 0.2‰. In tropical regions or where there is significant runoff or sea ice meltwater effects, local relationships that reflect the dominant freshwater source are likely to be more accurate.

The error in estimating the present-day calcification temperature is a combination of errors in core-top δ_c (σ_c), the assumed δ_w (σ_w), the temperature equation slope (σ_B), and the scatter of the temperature equation (σ_T)

$$\sigma_{T_c}^2 = \sigma_T^2 + B^2(\sigma_c^2 + \sigma_{\rm ml}^2) + (\delta_c - \delta_w)^2\sigma_B^2 \qquad (4)$$

(ignoring any error in the intercept), which gives (assuming that $\delta_c - \delta_w = O(2‰)$) $\sigma_{T_c} = 1.5$°C. If the error in the gradient of the temperature equation is excluded, the error reduces slightly to 1.4°C.

The calibration of T_c and the climatological temperature (that will be estimated from T_p) is generally a combination of offset and factor, i.e., $T_c = C + DT_p \pm \sigma_{\rm cal}$, although for simplicity, any difference between D and 1 is assumed to be negligible. Given the errors in estimating T_c, the scatter around any such calibration is likely to be of the same magnitude. Examples from the literature show that for *Neogloboquadrina pachyderma* (l) or *Globigerinoides bulloides*, simple offsets have been used to deduce T_c from summer SST (with scatter ± 1.2°–1.5°C) [*Duplessy et al.*, 1991]. In the tropics, *Globigerinoides ruber* (white) has been calibrated to to summer SST in the Atlantic (± 1.4°C) [*Wang et al.*, 1995] with a

combination of offset and factor, while in the Indian Ocean, *G. ruber* (white) has been calibrated with a simple offset (±1°C (estimated)) [*Rostek et al.*, 1993]. It is consistent with these results to assume a priori that the scatter in the calibration is of the same order as the error in calculating T_c, i.e. $\sigma_{\rm cal} \sim \sigma_{T_c}$. In actual cases, seasonality, depth stratification and regional differences will affect $\sigma_{\rm cal}$, and as in the Indian Ocean, the calibration error may well be smaller if circumstances are favorable.

3.5. Derive a δ_w Record From T_p and δ_c

Inverting (3) and substituting for T_c gives

$$\delta_w = \delta_c - \frac{1}{B}(T_p + C - A \pm \sigma_T \pm \sigma_{\rm cal})$$

Note that an additional 0.27‰ should be added to this value to convert the δ_w defined with respect to PDB to VSMOW. Combining the errors in δ_c T_p, the calibration and the temperature equation, the error in δ_w is

$$\sigma_w^2 = \sigma_c^2 + \frac{1}{B^2}(\sigma_{T_p}^2 + \sigma_T^2 + \sigma_{\rm cal}^2) \qquad (5)$$

An extra term of $[(T_p + C - A)/B^2]^2\sigma_B^2$ can also be included but is minor compared to the other errors. In the case where a calibration is necessary, $\sigma_w \sim 0.4$‰, and where no calibration is used, $\sigma_w \sim 0.25$‰.

3.6. Correct for Global Ice Volume Changes

Changes in sea level due to the growth and decay of ice sheets increase both global salinity and δ_w since the high latitude precipitation that forms the ice is very depleted (~ -30–-50‰). The changes in global mean salinity can be calculated as a function of mean sea level change: $\Delta S_m = 34.7\Delta/(3800 - \Delta)$ or more simply as $34.7\Delta/3800$ (to within 3%). Recent estimates of mean sea level change at the LGM are 120 ± 5 m (at Barbados) [*Fairbanks*, 1989] and 118 m [*Peltier*, 1998]. Since the latter number is tuned to the Barbados sea level curve the error in the sea level estimate is at least ±5 m. The change in δ_w is more difficult, and estimates at the LGM range from 1.0±0.1‰ [*Schrag et al.*, 1996] to 1.3‰ [*Fairbanks*, 1989]. The Fairbanks number is derived from a scaling with local sea level change (0.011‰ $\rm m^{-1}$ sea level change). The use of this scaling does involve an assumption that the increase of δ_w $\rm m^{-1}$ of sea level drop is invariant. Given the growth in elevation and general cooling that occur as the ice sheets grow, it might be expected that the increase should be greater for lower general sea level, but as yet, this effect is totally unquantified. Thus conservative estimates for the uncertainty in the ice volume change effects, S_i and δ_i, at the LGM are ∼0.05 and 0.1‰, respectively.

During times of rapid ice volume change the uncertainty must be greater since it is unclear exactly how the mean δ_w change propagates through the deep ocean. At timescales of $\lesssim$1000 years the deep ocean cannot be considered to be well mixed.

3.7. Assume the Paleo-δ_w:S Relationship

How can the uncertainties discussed in section 2 be quantified? The possible error in the global spatial gradient is governed by uncertainty in the net isotopic content of high-latitude precipitation δ_F (currently ~ -17‰). Since this must be $\gtrsim -10$‰ (the value of evaporation in the tropics, implying almost all precipitation falls in the high latitudes) and $\lesssim -30$‰ (the most depleted open ocean precipitation) the global gradient must be between ∼0.30 and 0.85. Neglecting a $(1 - S)$ factor, the paleo-mixing line is

$$\delta_w = \delta'_F + \left(\frac{\delta_i - \delta'_F}{S_m + S_i}\right) S \pm \sigma_{\rm ml}$$

$$= \delta'_F + G'S \pm \sigma_{\rm ml} \qquad (6)$$

where primed quantities represent the paleovalues. A standard error σ_F of 2‰ in the freshwater end-member corresponds to an error in the gradient of ∼0.06. Errors in the S_i and δ_i have only negligible effects on the global gradient error.

In the tropics, uncertainty in the isotopic content of the freshwater end-member will be less (since it will be close to the net evaporation value). However, the uncertainty may be greater in the Atlantic since the amount of water vapor exported to the Pacific could vary in time. The tropical mixing lines do not necessarily pass through mean ocean water; therefore an extra term $\delta_{\rm offset}$ (the offset in δ_w for tropical waters of mean ocean salinity compared to the mean ocean value) appears in the equation for G'. The error in assuming that this term remains constant in time will probably be small (<0.2‰), and so, it does not significantly contribute to the error. Local mixing line changes due to varying amounts of sea ice meltwater, river, or glacial runoff through time will increase the uncertainty but are harder to quantify in the absence of more detailed modeling.

3.8. Calculate S From δ_w

For the given δ_w the local paleosalinity is assumed to be on the estimated mixing line (6),

$$S = \frac{1}{G'}(\delta_w - \delta'_F \pm \sigma_{\rm ml}) \qquad (7)$$

The error in the absolute value of S is a combination of errors in $\delta_w(\sigma_w)$, the freshwater end-member (σ_F), the ice correction values and the goodness of fit of the mixing line ($\sigma_{\rm ml}$). However, since all possible lines are assumed to be passing through the mean ocean water the error is best represented as a function of $\Delta_{wi} = (\delta_w - \delta_i)/\delta'_F$ and after a number of small approximations have been made, is

$$\sigma_S^2 \sim \sigma_{S_i}^2 + \frac{1}{G^2}(\sigma_{\rm ml}^2 + \sigma_w^2 + \sigma_{\delta_i}^2 + \Delta_{wi}^2\sigma_F^2) \qquad (8)$$

This equation is valid for the tropics as well, with the understanding that σ_F corresponds to the uncertainty in the tropical freshwater end-member and that $\Delta_{wi} = (\delta_w - \delta_i - \delta_{\rm offset})/\delta'_F$.

3.9. Alternative Calibration to Present-Day Surface Salinity

The salinity deduced above is, at best, a measure of the salinity at the season and depth of calcification. Although corals and some tropical planktonic foraminifera do live exclusively in the mixed layer, other species, for example, *N. pachyderma* (l) and *G. bulloides*, have widely varying depth habitats and seasonal abundances [*Hemleben et al.*, 1989]. An alternative to calibrating the temperatures is a calibration of the core-top isotopic salinity to sea surface salinity. If the temperature calibration was purely an offset and the temperature equations are assumed to be linear, then this step oblivates the need for step 4, and T_p can be used directly in (3). *Wang et al.* [1995] performed a comparison between the summer salinity and the isotopic salinity deduced from core tops and showed a standard error of 0.7 and a significant offset of ∼2 . Essentially, this offset is a correction for the uncertainty in season and depth habitat and the possibly incorrect specification of the temperature equation or mixing line. However, this is not the standard error for all paleosalinity estimates due to ice volume effects and the uncertainty in the isotopic composition of the freshwater end-member. The error in the salinity changes is then the same as in (8) except that σ_w is now the uncalibrated value (0.25‰) and an extra error $\sigma_{S\rm cal}$ of ∼0.7 appears. Then σ_S is ∼1.1 (assuming σ_F = 2‰). This is slightly higher than for the temperature calibration method; however, the paleosalinity is calibrated directly to the surface salinity field.

4. Total Errors for Different Methodologies

Given perfect in situ temperature proxies and no errors in the ice volume change or mixing line gradient, the lowest error that is theoretically possible (given only the observed scatter in the global δ_w:S relationship and analytical measurement errors) is ∼0.45. In the tropics the reduced mixing line scatter ($\sigma_{\rm ml} = 0.13$) is roughly balanced by the increased error associated with the shallower gradient ($G = 0.3$), leaving the absolute minimum error about the same (0.5).

Table 1 shows the errors in δ_w and S associated with different temperature proxies calculated using the equations above. The difference between the various methods is substantial. Methods that use temperature proxies that record the in situ temperature at calcification lead to significantly smaller errors. In particular, the use of Mg/Ca or Sr/Ca ratios seems to have the best possibilities ($\sigma_S \sim$ 0.6–0.9) for reconstructing salinity changes.

For the reconstruction of paleosalinity through time and, in particular, at the LGM the uncertainties in the freshwater end-members and subsequent uncertainties in the δ_w:S mixing lines must be considered. Errors due to inaccuracies in the ice volume effects barely contribute to the overall error. Considering the global case first, LGM simulations using atmospheric general circulation models (AGCMs) with isotope tracers have produced high-latitude precipitation 4‰ [*Jouzel et al.*, 1994] and 6‰ [*Joussaume and Jouzel*, 1993] more depleted than at present. A reasonable guess might then be 5‰, although the uncertainty in this quantity could be O(2‰) or greater. Assuming that the gradient has remained invariant through time is equivalent to assuming that δ'_F was actually 1‰ greater at the LGM, well outside the error bars on the modeled values assumed here. As seen in (8), the influence of this error is dependent on how far away the estimated δ_w is from the ocean mean water (δ_i). Assuming differences to be of the order of 2‰ for a global reconstruction (though it may be less in more restricted domains), the σ_S at the LGM ranges from 0.8 to 1.2 (depending on the temperature proxy). For an uncertainty of 4‰ in δ'_F this increases to 1.1–1.5 . These are probably reasonable estimates

for the open-ocean midlatitudes. Where there may have been large changes in sea ice cover, for instance, in the northern North Atlantic, this is probably an underestimate.

For the tropics, modeling results from the LGM indicate that isotopic content of mean tropical precipitation increases only by the ice volume effect [*Jouzel et al.*, 1994]. In different ocean basins the increase in the average tropical precipitation is within $\delta_i \pm 0.5$ (bigger increases in the Pacific, smaller in the Indian, and average in the Atlantic). Hence an estimate for a basin-specific uncertainty σ_F could be 0.5‰. The range of δ_w in the tropics is less than for the global ocean, ∼0.5‰. Hence the freshwater end-member contribution to the total error is very small (less than even the ice volume uncertainty effect). Neglecting any changes in the difference between mean tropical water and the global mean leads to an error estimate of between 1.0 and 1.8‰ in the derived LGM tropical salinity. The errors are larger for the tropical salinities despite the greater confidence in the freshwater end-member because the slope of the δ_w:S relationship is shallower than in the midlatitudes. Errors in the calculated δ_w therefore cause proportionately more error in the salinity.

If many points are being considered and a pattern of change emerges (either at a single time slice with many points or over a substantial time interval at a single point), the error in the salinity difference reduces by a factor of $1/\sqrt{n}$, where n is the number of points. For example, the error in a mean change of salinity over 10 points decreases by a factor of 3, though this will only true if the estimates at each point are truly independent.

All of the error values have been calculated as standard deviations on the absolute numbers. Since these absolute numbers might well have a significant offset from the actual numbers and in order to remove systematic errors in any intercept values, salinity differences should be considered instead. However, while this eliminates this source of error, it does increase the scatter by a factor of $\sqrt{2}$. Our best estimate of the error in LGM open-ocean salinity differences is ∼1.1 (1.5 in the tropics) using the best proxies (1.7–2.5 for the worst). For statistical significance, differences should be $\gtrsim 2\sigma$; hence it could be argued that any signals in the paleosalinity $\lesssim$2 cannot be considered conclusive.

5. Conclusions

This paper has demonstrated that previously published error estimates of paleosalinities may be significantly underestimated. While this is not a significant problem for tracking the rough position of an important salinity front (for instance, in the North Atlantic) or for assessing a pattern of change, it may prove important for ocean modeling studies of past climates. Given the sensitivity of ocean models to even modest changes in the surface restoring salinity ($\lesssim$0.5), this analysis does not lend support to the use of paleosalinity fields as a boundary condition for ocean models.

The most serious sources of error occur because of the calibrations necessary to derive the calcification temperature from the proxy and because of the uncertainty in the freshwater end-member in the global δ_w:S mixing line. Better in situ proxies such as Mg/Ca ratios and better modeling of paleohydrologic cycles would seem to offer the best hopes for reducing these errors. It should be pointed out that at times of rapid climate change, such as the last deglaciation, it is quite probable that spatial and temporal variations in the mixing lines were much more severe than can be accounted for here. One procedure that may reduce the uncertainty is the use of δ_w as an independent tracer in GCM simulations of paleoclimate as called for by *Rohling and Bigg* [1998]. This should allow for better consistency checks between the simulated climates the proxy records.

What are the error bars on these error bars? Despite my best efforts it is completely possible that in some steps the likely errors have been overestimated or the possible cancelations of error have been underestimated. However, this paper provides an outline into which any quantitative improvements in technique or accuracy can easily be placed.

Acknowledgments. This analysis was helped by conversations with J. Lynch-Stieglitz, D. Lea, and J. Ortiz among others and by comments from S. D'Hondt and an anonymous reviewer. Many thanks also to D. Rind and G. Russell for their support. This work was done with the support of a NOAA Postdoctoral Fellowship in Climate and Global Change administered by the UCAR Visiting Scientist Program.

References

Bauch, D., P. Schlosser, and R. G. Fairbanks, Freshwater balance and the sources of deep and bottom waters

in the Arctic Ocean inferred from the distribution of $H_2^{18}O$, *Prog. Oceanogr.*, *35*, 53–80, 1995.

Bemis, B. E., H. J. Spero, J. Bijma, and D. W. Lea, Reevaluation of the oxygen isotopic composition of planktonic foraminifera: Experimental results and revised paleotemperature equations, *Paleoceanography*, *13*, 150–160, 1998.

Craig, H., and L. I. Gordon, Deuterium and oxygen 18 variations in the ocean and the marine atmosphere, in *Stable Isotopes in Oceanographic Studies and Paleotemperatures*, edited by E. Tongiorgi, pp. 9–130, Cons. Naz. di Rech., Spoleto, Italy, 1965.

Duplessy, J.-C., A. W. H. Bé, and P. L. Blanc, Oxygen and carbon isotopic composition and biogeographic distribution of planktonic foraminifera in the Indian Ocean, *Palaeogeogr. Palaeoclimatol. Palaeoecol.*, *33*, 9–46, 1981.

Duplessy, J.-C., L. Labeyrie, A. Juillet-Leclerc, F. Maitre, J. Duprat, and M. Sarnthein, Surface salinity reconstruction of the North Atlantic Ocean during the Last Glacial Maximum, *Oceanol. Acta*, *14*, 311–324, 1991.

Fairbanks, R. G., The origin of continental shelf and slope water in the New York Bight and Gulf of Maine, *J. Geophys. Res.*, *87*, 5796–5808, 1982.

Fairbanks, R. G., A 17,000-year glacio-eustatic sea level record: Influence of glacial melting rates on the Younger Dryas event and deep ocean circulation, *Nature*, *342*, 637–642, 1989.

Fairbanks, R. G., C. D. Charles, and J. D. Wright, Origin of global meltwater pulses, in *Radiocarbon After Four Decades: An Interdisciplinary Perspective*, edited by R. E. Taylor, A. Long, and R. S. Kra, pp. 473–500, Springer-Verlag, New York, 1992.

Gagan, M. K., L. K. Ayliffe, D. Hopley, J. A. Cali, G. E. Mortimer, J. Chappell, M. T. McCulloch, and M. J. Head, Temperature and surface-ocean water balance of the Mid-Holocene Tropical West Pacific, *Science*, *279*, 1014–1018, 1998.

Hastings, D. W., A. D. Russell, and S. R. Emerson, Foraminiferal magnesium in *Globigerinoides sacculifer* as a paleotemperature proxy, *Paleoceanography*, *13*, 161–169, 1998.

Hemleben, C., M. Spindler, and O. R. Anderson, *Modern Planktonic Foraminifera*, Springer-Verlag, New York, 1989.

Joussaume, S., and J. Jouzel, Paleoclimatic tracers: An investigation using an atmospheric general circulation model under ice age conditions, 2, Water isotopes, *J. Geophys. Res.*, *98*, 2807–2830, 1993.

Jouzel, J., R. D. Koster, R. J. Suozzo, and G. L. Russell, Stable water isotope behaviour during the Last Glacial Maximum: A general circulation model analysis, *J. Geophys. Res.*, *99*, 25,791–25,801, 1994.

Kim, S.-T., and J. R. O'Neil, Equilibrium and nonequilibrium oxygen isotope effects in synthetic carbonates, *Geochim. Cosmochim. Acta*, *61*, 3461–3475, 1997.

Macdonald, R. W., D. W. Paton, E. C. Carmack, and A. Omstedt, The freshwater budget and under-ice spreading of Mackenzie River water in the Canadian Beaufort Sea based on salinity and $^{18}O/^{16}O$ measurements in water and ice, *J. Geophys. Res.*, *100*, 895–919, 1995.

Muller, P. J., G. Kirst, G. Ruhland, I. von Stroch, and A. Rosell-Melé, Calibration of the alkenone paleotemperature index $U_{37}^{K'}$ based on core-tops from the eastern South Atlantic and the global ocean 60°N–60°S, *Geochim. Cosmochim. Acta*, *62*, 1757–1772, 1998.

O'Neil, J. R., R. N. Clayton, and T. K. Mayeda, Oxygen isotope fractionation in divalent metal carbonates, *J. Chem. Phys*, *51*, 5547–5558, 1969.

Ortiz, J. D., and A. C. Mix, Comparison of Imbrie-Kipp transfer function and modern analog temperature estimates using sediment trap and core-top foraminiferal faunas, *Paleoceanography*, *12*, 175–190, 1997.

Östlund, H. G., H. Craig, W. S. Broecker, and D. Spenser, GEOSECS Atlantic, Pacific and Indian Ocean expeditions, vol. 7, Shorebased data and graphics, *Tech. Rep.*, Nat. Sci. Found., Washington D.C., 1987.

Peltier, W. R., "Implicit ice" in the global theory of glacial isostatic adjustment, *Geophys. Res. Lett.*, *25*, 3955–3958, 1998.

Press, W. H., B. P. Flannery, S. A. Teukolsky, and W. T. Vetterling, *Numerical Recipes*, Cambridge Univ. Press, New York, 1990.

Rohling, E. J., and G. R. Bigg, Paleosalinity and $\delta^{18}O$: A critical assessment, *J. Geophys. Res.*, *103*, 1307–1318, 1998.

Rohling, E. J., and S. D. Rijk, Holocene climate optimum and Last Glacial Maximum in the Mediterranean: The marine oxygen isotope record, *Mar. Geol.*, *153*, 57–75, 1999.

Rostek, F., G. Ruhland, F. C. Bassinot, P. J. Müller, L. D. Labeyrie, Y. Lancelot, and E. Bard, Reconstructing sea surface temperature and salinity using $\delta^{18}O$ and alkenone records, *Nature*, *364*, 319–321, 1993.

Schmidt, G. A., Oxygen-18 variations in a global ocean model, *Geophys. Res. Lett.*, *25*, 1201–1204, 1998.

Schrag, D. P., G. Hampt, and D. W. Murray, Pore fluid constraints on the temperature and oxygen isotopic composition of the glacial ocean, *Science*, *272*, 1930–1932, 1996.

Spero, H. J., J. Bijma, D. W. Lea, and B. E. Bemis, Effect of seawater carbonate concentration on foraminiferal carbon and oxygen isotopes, *Nature*, *390*, 497–500, 1997.

Wang, L., M. Sarnthein, J.-C. Duplessy, H. Erlenkeuser, S. Jung, and U. Pflaumann, Paleo sea-surface salinities in the low-latitude Atlantic: The δ^{18}O record of *Globigerinoides ruber* (white), *Paleoceanography*, *10*, 749–761, 1995.

Weber, J. N., and P. M. J. Woodhead, Temperature dependence of oxygen-18 concentrations in reef coral carbonates, *J. Geophys. Res.*, *77*, 463–473, 1972.

Wellington, G. M., R. B. Dunbar, and G. Merlen, Calibration of stable oxygen isotope signatures in Gálapagos corals, *Paleoceanography*, *11*, 467–480, 1996.

G. A. Schmidt, NASA Goddard Institute for Space Studies and Center for Climate Systems Research, Columbia University, 2880 Broadway, New York, NY 10025. (gschmidt@giss.nasa.gov)

Received October 13, 1998; revised January 25, 1999; accepted January 31, 1999.

This preprint was prepared with AGU's LaTeX macros v5.01. File paper formatted May 18, 1999.

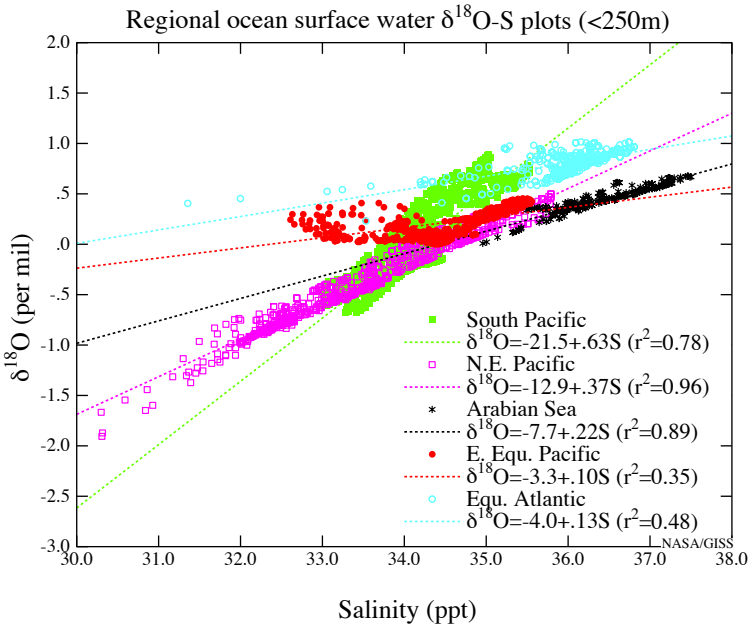

Figure 1. Spread of regional δ_w:S mixing lines in modeled output from Schmidt (submitted manuscript, 1999). The lines in the tropics are significantly shallower than those from higher latitudes, varying as a function of the evaporation/precipitation balance. Slopes are consistent with observed values (Arabian Sea, 0.28 [*Rostek et al.*, 1993]; equatorial Atlantic, 0.11; and South Pacific, 0.68 [*Craig and Gordon*, 1965])

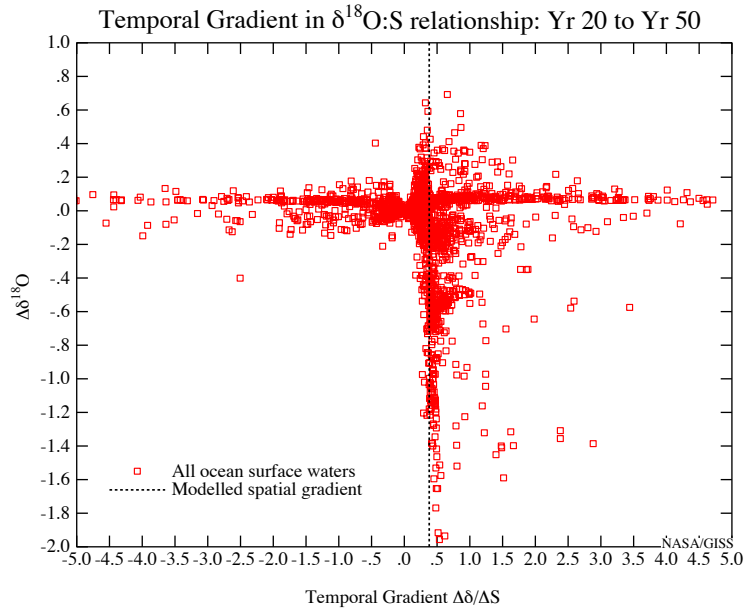

Figure 2. Temporal gradients ($\Delta\delta_w/\Delta S$) as a function of the magnitude of $\Delta\delta_w$ over a 30 year period in output from Schmidt (submitted manuscript, 1999). Note that for small variations in δ_w (<0.2) the temporal gradient is unrelated to the modeled spatial gradient (which does not change over this period).

Table 1. Errors Associated With Various Methodologies

Carbonate Source	Temperature Proxy	σ_{T_p} °C	σ_T °C	$\sigma_{\rm cal}$,[a] °C	σ_w,[b] ‰	Global Error,[c] σ_S	Tropical Error,[d] σ_S
Foraminifera	transfer functions	1.9	0.8	1.5	0.52	1.1	1.8
Foraminifera	modern analogs	1.5	0.8	1.5	0.46	1.0	1.6
Foraminifera	alkenone ratios	1.0	0.8	1.0	0.41	0.9	1.4
Foraminifera	Mg/Ca ratios	1.3	0.8	-	0.32	0.8	1.2
Corals	Sr/Ca ratios	1.0	0.5	-	0.23	0.6	0.9

Errors are calculated assuming no uncertainty in the ice volume effect or the freshwater end-member. The absolute minimum values of σ_w and σ_S, given the accuracy of the mixing lines and assuming only measurement errors are 0.1‰ and 0.45, respectively.

[a]Taken from previous publications. See text for sources.

[b]Calculated from (5).

[c]Calculated from (8) assuming $\sigma_{\rm ml} = 0.2$ and $G = 0.5$.

[d]Calculated from (8) assuming $\sigma_{\rm ml} = 0.13$ and $G = 0.3$.